World Academy of Science, Engineering and Technology
International Journal of Mechanical and Mechatronics Engineering
Vol:5, No:7, 2011

A Further Improvement on the Resurrected Core-Spreading Vortex Method

M-J. Huang*, C-J. Huang, L-C. Chen

***Abstract*—**In a previously developed fast vortex method, the diffusion of the vortex sheet induced at the solid wall by the no-slip boundary conditions was modeled according to the approximation solution of Koumoutsakos and converted into discrete blobs in the vicinity of the wall. This scheme had been successfully applied to a simulation of the flow induced with an impulsively initiated circular cylinder. In this work, further modifications on this vortex method are attempted, including replacing the approximation solution by the boundary-element-method solution, incorporating a new algorithm for handling the over-weak vortex blobs, and diffusing the vortex sheet circulation in a new way suitable for high-curvature solid bodies. The accuracy is thus largely improved. The predictions of lift and drag coefficients for a uniform flow past a NASA airfoil agree well with the existing literature.

***Keywords*—**Resurrected core-spreading vortex method, Boundary element method, Vortex sheet, Over-weak vortex blobs.

Open Science Index, Mechanical and Mechatronics Engineering Vol:5, No:7, 2011 publications.waset.org/2200/pdf

I. Introduction

THE resurrected core-spreading vortex method [1] captures correctly the diffusion phenomenon by linearly increasing the characteristic area of the Gaussian blobs [2] and imposing an upper bound on the characteristic area via a blob-splitting technique [3] [4]. To control the total number of vortex blobs, an algorithm was designed to merge similar and nearby vortices [4]. To speed up the calculation of the velocities, the multipole method was implemented [1]. This fast resurrected core-spreading vortex method is attractive because it is deterministic, grid-free, efficient, and exact for uniform flow fields, unlike those grid-based finite-difference methods (such as those described by Chang & Chern [5], Lu & Shen [6], and Lu & Ross [7]) that make the code no longer grid-free and might result in excessive interpolation errors or those redistribution methods (such as those proposed by Degond & Mas-Gallic [8], Fishelov (1990) [9], and Shankar & van Dommelen [10][11]) that rely strongly on the remeshing technique.

When the no-slip boundary conditions were present, the resurrected core-spreading vortex method [1] chose to place a vortex sheet at the wall and solve its strength with a boundary-element method and constant panels [12]; Koumoutsakos' analytical solution [13] was properly discretized to model the diffusion of the vortex sheet at a later time. When applied to the flow with an impulsively initiated circular cylinder, this vortex method performed excellently at early times but gradually lost its accuracy as the simulated time increased. A careful examination found two possible reasons. The first one involves the extremely weak vortex blobs that are generated after successive splitting processes and were deleted directly from the simulation. Without deleting these over-weak vortex blobs, the total number of vortex blobs blows up quickly however. The amount of circulation deleted accumulated with time and eventually caused unacceptable errors. The second reason is attributed to the employed constant panels that ignore the local curvature of the solid walls. In this work, the authors would like to explore these two error sources and possibly improve the accuracy. Flows past a NASA airfoil are targeted.

The resurrected core-spreading vortex method is briefly reviewed in Sec. II. The generation and diffusion of the vortex sheet on the solid wall are modeled in Sec. III. The over-weak vortex blobs are handled in Sec. IV. Simulation results of airfoil flows are presented in Sec. V. Finally given is the conclusion.

II. Resurrected Core-Spreading Vortex Method

The governing equation to be solved is

$$\frac{\partial \omega}{\partial t} + u\frac{\partial \omega}{\partial x} + v\frac{\partial \omega}{\partial y} = \nu \nabla^2 \omega \tag{1}$$

in which appear vorticity ω, velocity $\vec{u} = (u, v)$ and viscosity ν. The velocity is divided into two parts, one irrotational $\vec{u}_p$ and another rotational $\vec{u}_\omega$. According to Leonard's core-spreading method, the solution is decomposed into many discrete Gaussian blobs as follows

$$\omega(\vec{x}, t) = \sum_{j=1}^{N} \frac{\Gamma_j}{\pi \sigma_j^2} \exp\left(-\frac{\left|\vec{x} - \vec{x}_j\right|^2}{\sigma_j^2} \right) \tag{2}$$

in which appear location $\vec{x}_j$, core size σ_j and strength Γ_j of blob *j*; they are governed by

M-J. Huang is with Mechanical Engineering Department, National Taiwan University, Taipei, Taiwan (phone: 886-2-3366-2696; fax: 886-2-2363-1755; e-mail: mjhuang@ntu.edu.tw).
C.-J Huang is with Mechanical Engineering Department, National Taiwan University, Taipei, Taiwan (phone: 886-2-3366-4498; fax: 886-2-2363-1755; e-mail: b94202013@ntu.edu.tw).
L-C. Chen is with Mechanical Engineering Department, National Taiwan University, Taipei, Taiwan (phone: 886-2-3366-4498; fax: 886-2-2363-1755; e-mail: b91502126@ntu.edu.tw).
This work was supported by the National Science Council of Taiwan (Grant No. NSC 97-2221-E-002-200-MY3).

Open Science Index, Mechanical and Mechatronics Engineering Vol:5, No:7, 2011 publications.waset.org/2200/pdf

$$\frac{d\Gamma_j}{dt} = 0 \tag{3a}$$

$$\frac{d\sigma_j^2}{dt} = 4\nu \tag{3b}$$

$$\frac{d\vec{x}_j}{dt} = \vec{u}_p\left(\vec{x}_j, t\right) + \vec{u}_\omega\left(\vec{x}_j, t\right) \tag{3c}$$

The diffusion of Eq.(1) is simulated exactly with Eqs.(3abc) but not convection; the associated error increases with increasing σ_j [14]. As remedy, the core size must be kept small. It is done in the following way. A threshold $\sigma_{\max}$ for the core size is set first; whenever a blob has a core size σ_p greater than $\sigma_{\max}$, this blob is replaced immediately by a thinner one surrounded with *M* others. The core size of these new blobs is chosen to be $\alpha\sigma_p$ and their strengths are determined on preserving the zeroth, second, and fourth moments of vorticity. Physically, when diffusion is concerned, the vorticity at the original location decreases but always remains the maximum. The adopted splitting method approximates this major part of the vorticity with a blob of half the strength and a circumferential vorticity with the surrounding blobs so that it captures the diffusion more accurately [4].

As the duration of simulation increases, further splitting events occur, and the number of blobs increases rapidly. To contain this situation, similar (with the same sense of rotation) and nearby blobs should become merged into one. The strength (Γ_0), location, and core size (σ_0) of the new vortex blob are determined on preserving the zeroth, first and second moments of vorticity. By satisfying the two criteria

$$\Gamma_0 / \Gamma_{ref} < \pi\varepsilon\alpha^2\sigma_{\max}^2 \tag{4a}$$

$$\sigma_0 < \sigma_{\max} \tag{4b}$$

with selected error tolerance ε and reference circulation Γ_{ref}, the maximum field error induced in a single merging event is controlled with $\varepsilon\Gamma_{ref}$. The sets of similar and nearby blobs to be merged are determined as follows. The entire flow domain is divided into equal square cells of size $\eta\sigma_{\max}$, and the merging criteria are examined over blobs in each cell; at most one merging event is allowed per cell per time step. The distance between neighboring blobs after merging is thus about $\sqrt{2}\eta\sigma_{\max}$ (the diagonal distance of the cell). Because the minimum core size of a blob is $\alpha\sigma_{\max}$, the overlapping ratio (the ratio of the core size to the distance between neighboring blobs) is estimated to be $\alpha/\left(\sqrt{2}\eta\right)$ [4].

To speed up the calculations of velocities, the multipole method of Carrier et al. [15] was employed. Far-away blobs are viewed as point vortices, which contribution to the velocity of an interested blob is evaluated by a truncated Laurent series (*P* terms). The nearby blobs are grouped on taking advantage both of the square cells generated for merging similar and nearby blobs and of the concept of adaptive domain decomposition proposed by Carrier et al. [15]. Details about the grouping algorithm are referred to [1]. Errors of two kinds are associated with this fast method: the first arises from an approximation of vortex blobs by point sources, and the second is due to truncated terms of higher order. When the former dominates over the latter factor, increasing the counted terms cannot improve the accuracy but the computational amount. An optimized value of *P* was found to be [1]

$$P_{opt} = \frac{2l_{\min}^2}{\sigma^2} + 1 = \frac{2}{SR^2} + 1 \tag{5}$$

where $l_{\min}$ is the finest subdomain size involved with the adaptive domain decomposition and $SR \equiv \sigma / l_{\min}$. The fast vortex method is executed as follows. One first specifies the desired values of *SR* and n_0 (the maximum allowable number of vortex blobs in a group), then determines the truncated Laurent series according to Eq.(5), and finally sets the allowable maximum level for the domain decomposition as $\log_2\left(L \cdot SR/\sigma_{\max}\right)$, with *L* as the size of the minimum square that encloses all existing vortex blobs.

III. No-slip boundary conditions

The no-slip boundary condition is fulfilled on placing a vortex sheet of strength γ (circulation per unit length) at the wall. The strength is governed by

$$\gamma(s) - \frac{1}{\pi}\oint_S \frac{\partial}{\partial n}\log\left|\vec{x}(s) - \vec{x}(s')\right|\gamma(s')ds' = -2\frac{\partial \psi_{ext}}{\partial n}\left(\vec{x}(s)\right) \tag{6a}$$

$$\oint_S \gamma(s,t)\,ds + \Gamma_{wake}(t) = 0 \tag{6b}$$

in which ψ_{ext} is the stream function associated with the external flow, including free streams and vortex blobs, Γ_{wake} is the total circulation inside the flow, and *s* and *n* are tangential and normal coordinates along the solid boundary. We discretized Eq.(6) with the boundary-element method and constant panels (panels of constant strength) [12], and solved with a requirement of least squared error [16]. To avoid fluctuations, we treated the external vortex blobs as point vortices when evaluating the right side of Eq.(6a).

As time goes on, the circulation on the solid wall must gradually diffuse into the flow field. Due to the singularity, the diffusion can be approximated by

$$\frac{\partial \omega_\gamma}{\partial t} - \nu\nabla^2\omega_\gamma = 0 \tag{7a}$$

$$\omega_\gamma\left(\vec{x}, 0\right) = 0 \tag{7b}$$

$$\nu\frac{\partial\omega_\gamma}{\partial n}=-\frac{\gamma}{\delta t}\qquad\text{at the wall}\tag{7c}$$

The exact solution of Eq.(7) is known as follows: [13]

$$\omega_\gamma(\vec{x},t)=\int_0^t\oint_S G(\vec{x},t;\vec{x}'(s),\tau)\mu(s,\tau)\,ds\,d\tau\tag{8a}$$

$$-\frac{1}{2}\mu(s,t)+\oint_S\int_0^t\nu\frac{\partial G}{\partial n}(\vec{x}(s),t;\vec{x}(s'),\tau)\mu(s',\tau)\,ds'\,d\tau=\nu\frac{\partial\omega}{\partial n}\tag{8b}$$

where

$$G(\vec{x},t;\vec{x}',\tau)=\frac{1}{4\pi\nu(t-\tau)}\exp\left(-\frac{|\vec{x}-\vec{x}'|^2}{4\nu(t-\tau)}\right)\tag{8c}$$

Assuming a piecewise linear surface, extending the spatial integration to infinity, and approximating the time integration by the forward Euler method, Koumoutsakos proposed an approximation solution [13] as follows

$$\omega_\gamma(\vec{x},\delta t)=\sum_{i=1}^{M}\frac{1}{2}\{\mu_i\Phi_i(\vec{x},\delta t)\}\,\delta t\tag{9a}$$

$$\Phi_i(\vec{x},\delta t)=\frac{1}{\sqrt{4\pi\nu\delta t}}\cdot\exp\left(-\frac{(y-y_{c,i})^2}{4\nu\delta t}\right)\cdot\left\{erf\left(\frac{d_i-(x-x_{c,i})}{\sqrt{4\nu\delta t}}\right)+erf\left(\frac{d_i+(x-x_{c,i})}{\sqrt{4\nu\delta t}}\right)\right\}\tag{9b}$$

$$\mu_i\approx\frac{2\gamma_i}{\delta t}\tag{9c}$$

in which appear the midpoint ($x_{c,i}$, $y_{c,i}$) of the i[th] panel, time increment δt, panel strength γ_i, panel length d_i, the total number of panels M, and error function *erf*. Alternatively, one may solve μ_i (Eq.(8)) also by the boundary element method. We name these two methods as the linear method and the BE method. Comparisons will be made between their performances.

To discretize the vorticity distribution Eq.(9) and to be consistent with the resurrected core-spreading vortex method, new blobs, called *wall blobs*, are generated at selected locations outside the solid body (having a core size of σ_γ). In the work of Huang et al. [1], these blobs were placed along the curved surface and each panel distributed its circulation to the neighboring ten blobs (see Fig.1(a)) and, most of all, each five of them were treated as if they were collinear (see Fig.1(b)). This approximation however causes unacceptable errors when the body curvature (such as at the trailing edge of an airfoil) is huge. In the present work, we instead place ten blobs outside each panel independently as shown in Fig.2. Although the total number of wall blobs is increased, it is reduced shortly by the merging process and thus hardly increases the computational time.

IV. Other Numerical Issues

A. Vortex Blobs Near the Wall

During the simulation, some vortex blobs may move, because of convection or splitting, toward the wall and remain too close to the wall such that their Gaussian tails extend into the interior of the solid body, causing significant errors. To fix it, a blob satisfying the following criterion:

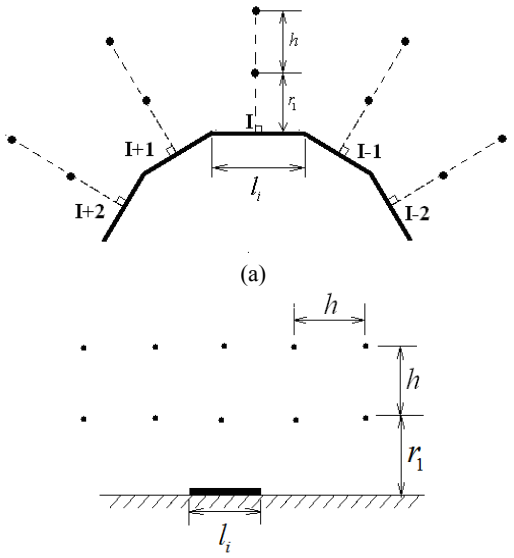


Fig.1 The old locations of the wall blobs created to approximate the diffusion result of the vortex sheet at the wall (a) and the collinear approximation (b).

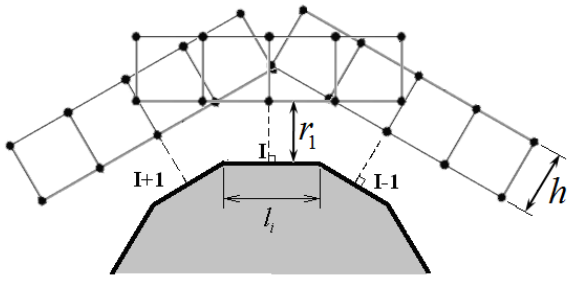


Fig.2 The new locations of the wall blobs created to approximate the diffusion result of the vortex sheet at the wall.

$$\frac{r}{\sigma}<\frac{r_1}{\sigma_\gamma}\equiv r^*\tag{10}$$

in which r is the distance from the wall and σ is the core size of the blob, is judged too close to the wall and will be eliminated from the simulation after it gives up its circulation to nearby wall blobs.

B. Over-weak Vortex Blobs

After successive splitting processes, there can appear a huge number of extremely weak vortex blobs. These blobs affect little the flow field but cost a huge amount of computations. In the previous solver [1], a threshold ($\Gamma_{\text{tolerance}}$) was prescribed and any blob which strength was smaller than this threshold

Open Science Index, Mechanical and Mechatronics Engineering Vol:5, No:7, 2011 publications.waset.org/2200/pdf

Open Science Index, Mechanical and Mechatronics Engineering Vol:5, No:7, 2011 publications.waset.org/2200/pdf

was deleted directly from the simulation. Error thus accumulates as time increases and eventually becomes unacceptable because of the abandonment of the circulation. As remedy, we herein distribute the circulation of any over-weak blob equally to its neighboring blobs before deleting it. The neighboring blobs are selected by taking advantage of the grid generated for merging similar and nearby blobs in the following order of priority: 1) blobs with the same sense of rotation and residing in the same cell as the over-weak blob does, 2) blobs with the same sense of rotation and within the 8 cells enclosing the cell the over-weak blob resides, and 3) blobs with the opposite sense of rotation and residing in the same cell as the over-weak blob does. Fig. 3 shows the drag coefficient of the flow induced with an impulsively initiated circular cylinder with $Re_D=UD/\nu= 3000$. The time increment is $\Delta t= 0.005$ and $\Gamma_{tolerance}=5\times10^{-7}UD$. The drag coefficient is computed as follows

$$I = \sum_{i=1}^{N} y_i \Gamma_i + \sum_{m=1}^{M} y_{c,m} \gamma_m d_m \tag{11a}$$

$$C_D = \frac{I(t-\delta t) - I(t+\delta t)}{U^2 D \delta t} \tag{11b}$$

where appears the total number of vortex blobs in the flow, *N*. Fig. 3 reveals a much better agreement between this modified scheme with Ploumhans and Winckelmans' [17] than the original one. The instantaneous vorticty contours at tU/D=5 are shown in Fig.4. Locations of over-weak vortex blobs at this time are also indicated. In the figure, blue dots are those blobs going to give up their circulations to other blobs in the same cell and green ones are those going to give up their circulations to blobs in the neighboring 8 cells.

V. NACA0012 Airfoil

We finally chose the NACA0012 airfoil to test the performance of the newly designed wall blobs, i.e. to test the capability of the modified solver in simulating flows over body with high curvature. Two angles of attack, 12° and 27°, were first simulated. Both have a Reynolds number of Re=Uc/ν=100, where c is the chord. The drag and lift coefficients were calculated after the simulations reached steady. The results are listed in Table I, compared with those of Srinath & Mittal [18]. The linear method seemingly performs better than the BE method. The errors are under 5%. Fig. 5 shows the steady vorticity distributions. Slight vortex shedding is observed when the angle is 27°; the oscillating amplitude in the drag/lift coefficient is still very small. The life and drag coefficients against the angle of attack are shown in Figs. 6 and 7 respectively. The present method predicts well in the lift coefficients, in agreement with those of Srinath & Mittal [18] but slightly over-predicts the drag coefficients.

VI. Conclusion

We improved the accuracy of an existing resurrected core-spreading vortex method and extended its applications to flows past solid bodies with high curvatures. The over-weak

TABLE I. The drag and lift coefficients calculated.

	Srinath & Mittal		linear		BE	
	C_D	C_L	C_D	C_L	C_D	C_L
12°	0.478	0.583	0.498	0.612	0.503	0.661
27°	0.667	0.815	0.686	0.806	0.682	0.798

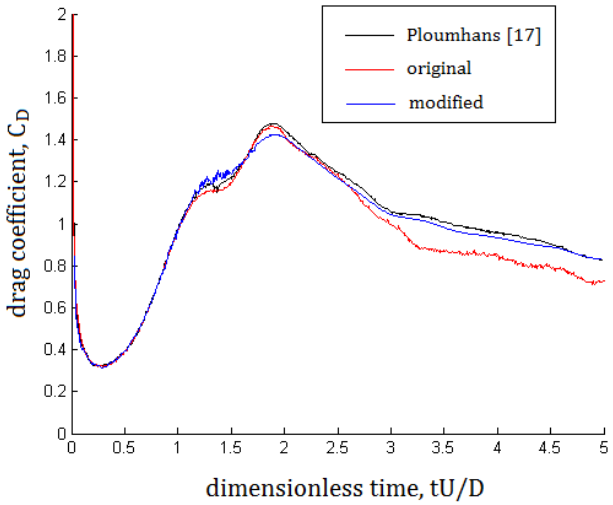


Fig.3 A comparison between the calculated drag coefficients.

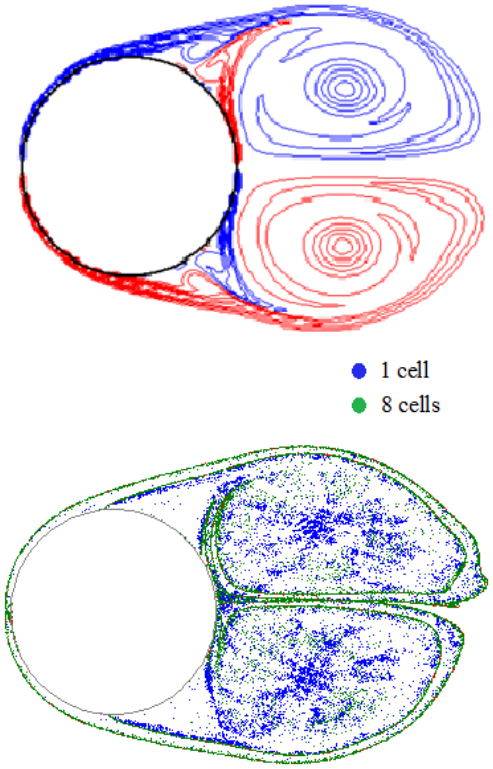


Fig.4 The vorticity contours and the distribution of the over-weak vortex blobs at tU/D=5.

Open Science Index, Mechanical and Mechatronics Engineering Vol:5, No:7, 2011 publications.waset.org/2200/pdf

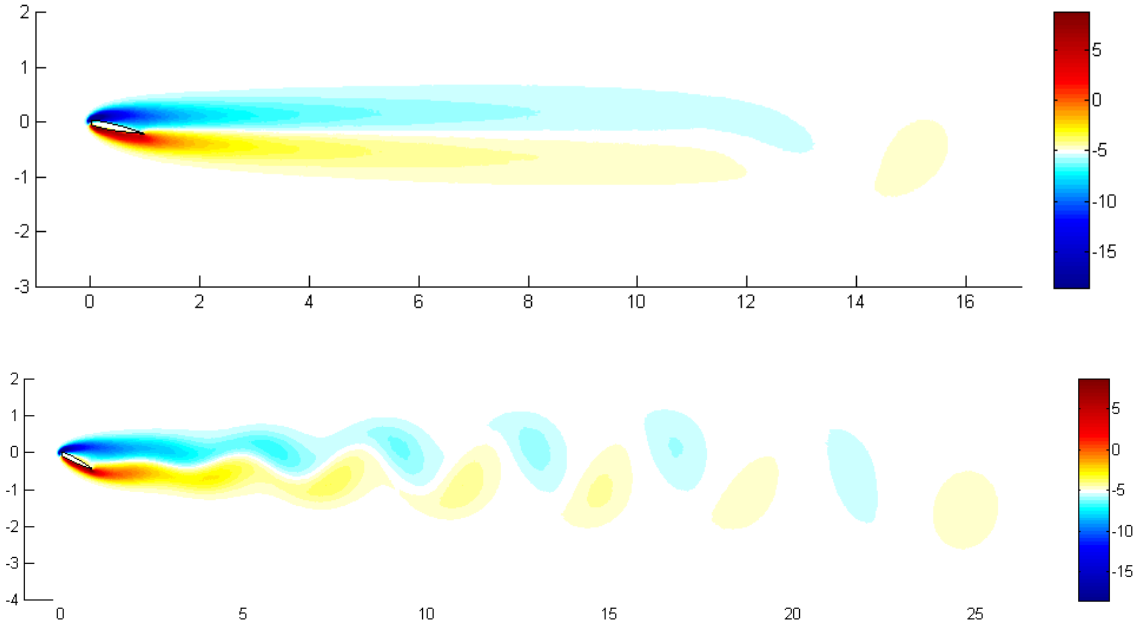


Fig. 5 The color contour of vorticity for a uniform flow past a NACA0012 airfoil. The angle of attack is 12° (top) and 27° (bottom).

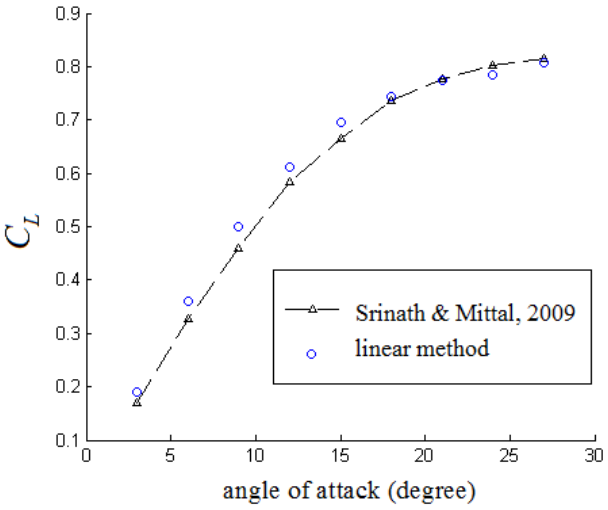


Fig. 6 The lift coefficient against the angle of attack for the NACA0012 airfoil.

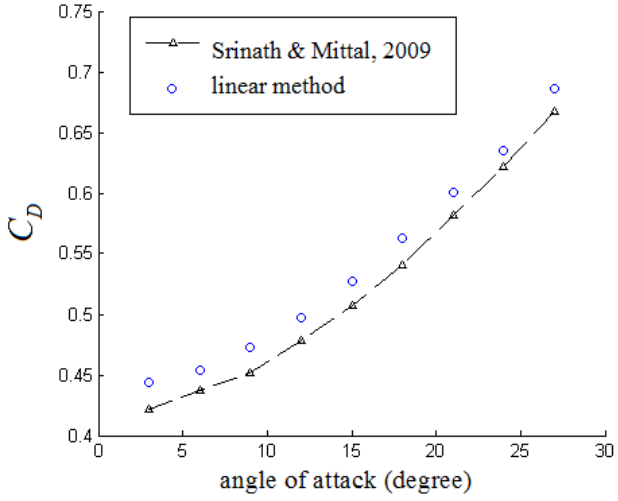


Fig.7 The drag coefficient against the angle of attack for the NACA0012 airfoil.

vortex blobs are not eliminated until their circulations are properly distributed to the neighboring blobs. The no-slip boundary conditions are satisfied by placing a vortex sheet on the solid wall, which strength is calculated by the boundary element method. The diffusion of this vortex sheet is either modeled by an approximation solution or solved by the boundary element method. The present study shows the former performs better and well in predicting the lift and drag coefficients for a uniform flow past a NASA airfoil with an angle of attack ranging from 3° to 27°.

REFERENCES

[1] M.J. Huang, H.X. Su, and L.C. Chen "A fast resurrected core-spreading vortex method with no-slip boundary conditions," J. Comput. Phys. 228, pp.1916-1931, 2009.

[2] A. Leonard, "Vortex methods for flow simulation," J. Comput. Phys. 37, pp.289-335, 1980.

[3] L. Rossi, "Resurrecting core spreading vortex methods: A new scheme that is both deterministic and convergent," SIAM J.Sci.Comp. 17, pp.370-397, 1996.

[4] M.J. Huang, "Diffusion via splitting and remeshing via merging in vortex method," Int. J. Numer. Meth. Fluids 48, pp.521-539, 2005.

[5] C. Chang and R. Chern, "A numerical study of flow around an impulsively started circular cylinder by a deterministic vortex method," J. Fluid Mech 223, pp.243-263, 1991.

[6] Z.Y. Lu and S.F. Shen, "Numerical Methods in Laminar and Turbulent Flow," Pineridge Press, Swansea, UK 5, p.619, 1987.
[7] Z.Y. Lu and T.J. Ross, "Diffusing-vortex numerical scheme for solving incompressible Navier–Stokes equations," J. Comput. Phys. 95, 1991, pp.400-435.
[8] P. Degond and S. Mas-Gallic, "The weighted particle method for convection–diffusion equations. Part 1: The case of an isotropic viscosity," Math. Comput. 53, pp. 485–507, 1989.
[9] D. Fishelov, "A new vortex scheme for viscous flow," J. Comput. Phys. 86, pp. 211–224, 1990.
[10] S. Shankar and L.L. van Dommelen, "A new diffusion procedure for vortex methods," J. Comput. Phys. 127, pp.88–109, 1996.
[11] L.L. Van Dommelen and S. Shankar, "Two counter-rotating diffusing vortices," Phys. Fluids A 7, pp. 808–819, 1995.
[12] Prem K. Kythe, "An introduction to boundary element methods," CRC Press, Boca Raton, 1995.
[13] P. Koumoutsakos, A. Leonard, and F. Pepin, "Boundary condition for viscous vortex methods," J. Comput. Phys. 113, pp.52–61, 1994.
[14] C. Greengard, "The core-spreading vortex method approximations the wrong equation," J. Comput. Phys. 61, pp.345 –348, 1985.
[15] J. Carrier, L. Greengard, and V. Rokhlin, "A fast adaptive multipole algorithm for particle simulations," SIAM J. Sci. Stat.Comput. 9, pp.669–686, 1988.
[16] N.R. Clarke, and O.R. Tutty, "Construction and validation of a discrete vortex method for the two-dimensional incompressible Navier–Stokes equations," Comput. Fluids 23, pp.751–783, 1994.
[17] P. Ploumhans and G.S. Winckelmans, "Vortex methods for high-resolution simulations of viscous flow past bluff bodies of general geometry," J. Comput. Phys. 165, pp.364–406, 2000.

Open Science Index, Mechanical and Mechatronics Engineering Vol:5, No:7, 2011 publications.waset.org/2200/pdf